Hindawi
Journal of Function Spaces
Volume 2023, Article ID 9077924, 10 pages
https://doi.org/10.1155/2023/9077924

Research Article

An Efficient and Robust Numerical Solver for Impulsive Control of Fractional Chaotic Systems

Zahra Moniri,[1] **Behrouz Parsa Moghaddam**,[2] **and Morteza Zamani Roudbaraki**[3]

[1]*Mathematics Department, University of Mazandaran, Babolsar, Iran*
[2]*Department of Mathematics, Lahijan Branch, Islamic Azad University, Lahijan, Iran*
[3]*Department of Computer, Lahijan Branch, Islamic Azad University, Lahijan, Iran*

Correspondence should be addressed to Behrouz Parsa Moghaddam; parsa@liau.ac.ir

Received 11 August 2022; Revised 20 December 2022; Accepted 13 April 2023; Published 4 May 2023

Academic Editor: Jia-Bao Liu

This paper derives a computationally efficient and fast-running solver for the approximate solution of fractional differential equations with impulsive effects. In this connection, for approximating the fractional-order integral operator, a B-spline version of interpolation by corresponding equal mesh points is adopted. An illustrative example illustrates the accuracy of the new solver results as compared with those of the previous study. The proposed solver's performance is evaluated by the fractional Rössler and susceptible-exposed-infectious impulsive systems. Moreover, the effect of impulsive behaviors is shown for various values of impulsive.

1. Introduction

The impulsive differential equations (IDEs) are mostly investigated systems together with short-time perturbations [1–4]. Impulsive control systems have been studied in many fields such as economics [5], chemostat [6], population ecology [7, 8], engineering [9], and neural networks [10, 11]. Many theoretical and numerical researchers have investigated IDEs in many studies. In [12–15], the existence and uniqueness theorems on IDEs have been analyzed. In addition, analytical and numerical solutions of this kind of equation have been investigated in [16–21] and etc.

Nowadays, one of the most famous branches of mathematical science is the fractional calculus with arbitrary fractional order [22]. The fractional calculus is applied to the model of many phenomena including control [23], mechanics [24], physics [25–27], stock market [28], electronics [29], biology [30], and epidemiology [31, 32]. Recently, fractional impulsive differential equations (FIDEs) are considered in simulations of many systems including chaotic and hyperchaotic systems [33–35], control [36], and neural networks [37]. The existence of the solutions of FIDEs is studied in [38] by using the fixed point method. The existence of solutions for FIDEs with the integral jump and antiperiodic conditions is investigated in [39]. Furthermore, the existence of solutions of these equations is analyzed through a global bifurcation approach in [40]. The existence and stability results are presented in [41].

To the best of the author's knowledge, developing a fast-running solver requires FIDE up to date. This motivates our interest to designate an accurate computational technique for solving the following FIDE:

$$\begin{aligned} {}^{C}\mathscr{D}^{\beta}_{0,t}u(t) - Q(t,u(t)) &= 0, \quad t \in \Upsilon' \coloneqq \Upsilon \setminus \mathscr{T}, \\ \Delta u(t) = u(t_n^+) - u(t_n) &= K_n(u(t_n)), \quad n = 1, 2, \cdots, i, i \in \mathbb{N} \\ u(0^+) &= u_0, \end{aligned} \tag{1}$$

where $0 < \beta < 1$, $Y \coloneqq [0, T]$, $\mathscr{T} \coloneqq \{t_1, t_2, \cdots, t_i\}$, where every t_n satisfies $0 = t_0 < t_1 < \cdots < t_i < t_{i+1} = T$, and plus $Q : Y \times = R \longrightarrow = R$ is jointly continuous function. Moreover, $K_n \coloneqq R \longrightarrow = R$, and $i = [T/\tau]$, where $\tau = t_{i+1} - t_i$ denotes the impulsive interval. Furthermore, $u(t_n^-) = \lim_{\varepsilon \longrightarrow 0^-} u(t_n + \varepsilon)$ and $u(t_n^+) = \lim_{\varepsilon \longrightarrow 0^+} u(t_n + \varepsilon)$ indicate the left and right limits of $u(t)$ at $t = t_n$, respectively.

Throughout this paper, we do choose the Riemann-Liouville fractional integral [42] and fractional derivative in the Caputo sense [43, 44] which are formulated as

$$\begin{aligned} \mathscr{J}^{\beta}_{0,t}u(t) &= \frac{1}{\Gamma(\beta)}\int_0^t u(\varsigma)(t-\varsigma)^{\beta-1}d\varsigma, \\ {}^{C}\mathscr{D}^{\beta}_{0,t}u(t) &= \frac{1}{\Gamma(p-\beta)}\int_0^t \frac{u^{(p)}(\varsigma)}{(t-\varsigma)^{\beta+1-p}}d\varsigma, \quad p \in = N, \end{aligned} \tag{2}$$

where t, $\beta, \varsigma \in = R^{+}$ and $p-1<\beta\le p$. In addition, the unknown function, $u(t)$, is continuously differentiable $(p-1)-$ times.

The rest of the paper is arranged as follows. Section 2 suggests an implicit numerical technique, by using base spline interpolation for discretizing the FIDE. Section 3 investigates the performance and accuracy of the new solver by analysing the fractional impulsive Rössler and SEI systems. To sum up, Section 4 proffers the concluding remarks and statements.

2. Theoretical Argument

The proposed benefits of this section are twofold:

(1) It gives a fractional order approximation of the integral nonlocal operators

(2) It provides an accurate and computationally efficient technique for solving FIDE (1)

Thereafter, we consider that $t_m = m\hbar$, $m=\{0,1,\cdots,r\}$, and $\hbar=[T/r]$ means the uniform step size, and $r \in = N$.

Proposition 1. *Assume that $u(t)\in C^2(Y)$ be a function, $\beta>0$ and $\|u^{(2)}(t)\|_{\infty}\le M$, where $M>0$. The approximation of the nonlocal integral, $\mathscr{J}^{\beta}_{0,t_r}[u(t)]$, using the B-spline interpolation can be stated as follows:*

$$\mathscr{J}^{\beta}_{0,t_r}[u(t)] \approx \sum_{m=0}^{r} a_{m,r}u_m \equiv \left(\mathscr{J}^{\beta}_{0,t_r}[u(t)]\right)_{approx}, \tag{3}$$

where

$$\begin{aligned} a_{m,r} &= \frac{\hbar^{\beta}}{\Gamma(\beta+2)} \\ &\times \begin{cases} (r-1)^{\beta+1}-(r-\beta-1)(r)^{\beta}, & m=0, \\ (r-m+1)^{\beta+1}+(r-m-1)^{\beta+1}-2(r-m)^{\beta+1}, & 1\le m\le r-1, \\ 1, & m=r. \end{cases} \end{aligned} \tag{4}$$

In addition, the truncation error of (3) is

$$\left\|\mathscr{J}^{\beta}_{0,t_r}[u(t)]-\left(\mathscr{J}^{\beta}_{0,t_r}[u(t)]\right)_{approx}\right\|_{\infty} \le \frac{r^{\beta}M}{8\Gamma(\beta+1)}\hbar^{2+\beta}. \tag{5}$$

Proof. The $u(t)-$ approximation function, $S_m(t)$, in $[t_m, t_{m+1}]\subseteq \mathscr{T}$; $m=0,1,\cdots,r-1$, by considering the B-spline interpolation is stated as

$$u_m(t)\approx S_m(t)=\left(\frac{t-t_m}{t_{m+1}-t_m}\right)u(t_{m+1})+\left(\frac{t-t_{m+1}}{t_m-t_{m+1}}\right)u(t_m). \tag{6}$$

Substituting (6) into (2), we obtain the time discretization form of (2) as follows:

$$\begin{aligned} \mathscr{J}^{\beta}_{0,t_r}[u(t)] &\approx \int_{0+}^{t_r}\frac{1}{\Gamma(\beta)}S_m(\zeta)(t_r-\zeta)^{\beta-1}\mathrm{d}\zeta \\ &= \sum_{m=0}^{r-1}\left(\int_{t_m}^{t_{m+1}}\frac{(t_r-\zeta)^{\beta-1}}{\Gamma(\beta)}\frac{\zeta-t_{m+1}}{t_m-t_{m+1}}\mathrm{d}\zeta\right)u(t_m) \\ &\quad+\sum_{m=0}^{r-1}\left(\int_{t_m}^{t_{m+1}}\frac{(t_r-\zeta)^{\beta-1}}{\Gamma(\beta)}\frac{\zeta-t_m}{t_{m+1}-t_m}\mathrm{d}\zeta\right)u(t_{m+1}). \end{aligned} \tag{7}$$

After rearranging and simplifying the above equation, it leads to (3) where the coefficients $a_{m,r}$ are given by (4).

Subsequently, the B-spline interpolation polynomial $S_m(t)$ satisfies

$$\mathscr{E}_m(t) \coloneqq u_m(t)-S_m(t)=(t-t_m)(t-t_{m+1})\frac{u''(\eta_m)}{2}, \tag{8}$$

where $\eta_m\in(t_m,t_{m+1})$ and $\mathscr{E}_m(t)$ denote error function. Therefore, we have

$$\begin{aligned} &\left\|\mathscr{J}^{\beta}_{0,t_r}[u(t)]-\left(\mathscr{J}^{\beta}_{0,t_r}[u(t)]\right)_{\text{approx}}\right\|_{\infty} \\ &=\frac{1}{\Gamma(\beta)}\int_0^{t_r}\left\|(t_r-\varsigma)^{\beta-1}\mathscr{E}(\varsigma)\right\|_{\infty}d\varsigma \\ &=\frac{1}{\Gamma(\beta)}\sum_{m=0}^{r-1}\int_{t_m}^{t_{m+1}}(t_r-\varsigma)^{\beta-1}\left\|\frac{u''(\eta_m)}{2}(t-t_m)(t-t_{m+1})\right\|_{\infty}d\varsigma \\ &\le\frac{M}{8\Gamma(\beta)}\hbar^2\sum_{m=0}^{r-1}\int_{t_m}^{t_{m+1}}(t_r-\varsigma)^{\beta-1}d\varsigma=\frac{t_r^{\beta}M}{8\Gamma(\beta+1)}\hbar^2 \\ &=\frac{r^{\beta}M}{8\Gamma(\beta+1)}\hbar^{\beta+2}. \end{aligned} \tag{9}$$

□

In the rest of this section, we designate a fast-running technique for solving FIDE (1) by means of Proposition 1. FIDE (1) is able to state the following two equivalent equations with the same solutions:

$$u(t)=u_0+\sum_{j=1}^{n}K_j(u_j)+\mathscr{J}^{\beta}_{0,t}Q(t,u(t)), \quad n=1,2,\cdots,i \tag{10}$$

or

$$u(t) = \begin{cases} u_0 + \dfrac{1}{\Gamma(\beta)} \displaystyle\int_0^t Q(\varsigma, u(\varsigma))d\varsigma, & t \in [0, t_1], \\ u_0 + K_1(u_1) + \dfrac{1}{\Gamma(\beta)} \displaystyle\int_0^t Q(\varsigma, u(\varsigma))d\varsigma, & t \in (t_1, t_2], \\ \vdots & \vdots \\ u_0 + \displaystyle\sum_{j=1}^{i} K_j(u_j) + \dfrac{1}{\Gamma(\beta)} \displaystyle\int_0^t Q(\varsigma, u(\varsigma))d\varsigma, & t \in (t_i, T]. \end{cases} \tag{11}$$

By using the presented approximation in Proposition 1, we get the following approximation:

$$\mathcal{J}^{\beta}_{0,t_r} Q(t, u(t)) \approx \sum_{m=0}^{r} a_{m,r} Q(t_m, u_m). \tag{12}$$

Therefore, by replacing (12) with (10) (or (11)), the following equation derives

$$u_r = u_0 + \sum_{j=1}^{i} K_j(u_j) + \sum_{m=0}^{r} a_{m,r} Q(t_m, u_m), \tag{13}$$

where $a_{m,r}$ is given by (4). Due to the nonlinear source term $Q(t, \cdot)$, we have

$$u_r^p = u_0 + \frac{\hbar^{\beta}}{\Gamma(\beta+1)} \sum_{m=0}^{r-1} b_{m,r} Q(t_m, u_m), \tag{14}$$

where

$$b_{m,r} = (r-m)^{\beta} - (r-m-1)^{\beta}, 0 \le m \le r-1. \tag{15}$$

Ultimately, replacing u_r^p in the righthand side of (13) yields

$$u_r = u_0 + \sum_{j=1}^{i} K_j(u_j) + Q(t_r, u_r^p) + \sum_{m=0}^{r-1} a_{m,r} Q(t_m, u_m). \tag{16}$$

3. Numerical Application and Discussion

This section evaluates the accuracy and computational efficiency of the proposed numerical technique. To evaluate the computational impact of this solver, the mean absolute error ($\mathscr{E}_M$),

$$\mathscr{E}_M = \frac{1}{M} \sum_{m=1}^{M} \mathrm{AE}_m, \tag{17}$$

where $\mathrm{AE}_m = |\mathcal{J}^{\beta}_{0,t_m}[u(t)] - (\mathcal{J}^{\beta}_{0,t_m}[u(t)])_{\mathrm{approx}}|$ and M represents the number of interior mesh points, and the convergence order ($\mathscr{C}_{h,M}$)

$$\mathscr{C}_{h,M} = \log_{\hbar}(\mathscr{E}_M) \tag{18}$$

is considered evaluation criteria. All the computational results are implemented with MATLAB R2019a on an AMD Ryzen 7 5700 U @ 1.80 GHz machine. Furthermore, a comparison is made with the IM algorithm that was formulated and investigated in [45, 46].

Example 2. Let $u(t) = \pi t \sin(\pi t)$. Then, we get

$$\mathcal{J}^{\beta}_{0,t}[u(t)] = \frac{-(\beta+2)}{\pi^{1/2+\beta}\sqrt{t}\Gamma(3+\beta)} \cdot \left((t^2\pi^2 + \beta) S_{3/2+\beta,1/2}(\pi t) + \beta^2\pi^2 t S_{1/2+\beta,3/2}(\pi t) - (\pi t)^{5/2+\beta} \right), \tag{19}$$

where $\beta > 0$ and $S_{\eta,\nu}(t)$ define the Lommel function as

$$S_{\delta,\varrho}(t) = t^{\delta+1} \frac{{}_1F_2\left([1]; [1/2(\delta-\varrho+3), 1/2(\delta+\varrho+3)]; (-1/4)t^4\right)}{(\delta+1)^2 - \varrho^2}, \tag{20}$$

where ${}_sF_d(u_1, \cdots, u_s; v_1, \cdots, v_d; t)$ defines the generalized hypergeometric function.

The performance of the presented method is described by $\mathcal{J}^{\beta}_{0,t}[\pi t \sin(\pi t)]$ in Example 2 which is shown in Table 1. Table 1 shows the values of $\mathscr{E}_M$, $\mathscr{C}_{h,M}$, and computational times of Equation (19) with $\hbar = \{0.01, 0.005, 0.002\}$ and $\beta = \{0.4, 0.7, 0.9\}$ in the interval $t \in [0, 1]$. The numerical results display the improved accuracy of the presented scheme compared to the IM scheme [45] in the viewpoint of the $\mathscr{E}_M$, $\mathscr{C}_{h,M}$, and computational times. Figure 1 depicts the curves of Equation (19) for $\beta = \{0.1, 0.2, \cdots, 1\}$ with step size $\hbar = 0.01$. The outcomes in Figure 1 and Table 1 show that the proposed scheme is more accurate and has less computational time than the IM scheme [45].

3.1. Application of the Suggested Solver. In this section, the performance of the suggested solver is investigated for FIDEs.

Application 3. The fractional Rössler system is stated as

$$\begin{aligned} {}^{C}\mathcal{D}^{\beta_1}_{0,t} x(t) &= -(y(t) + z(t)), \\ {}^{C}\mathcal{D}^{\beta_2}_{0,t} y(t) &= x(t) + \alpha y(t), \\ {}^{C}\mathcal{D}^{\beta_3}_{0,t} z(t) &= (x(t) - \theta) z(t) + \chi, \\ x(0) = x_0, y(0) &= y_0, z(0) = z_0, \end{aligned} \tag{21}$$

where $2 \le \theta \le 11$ and $0 < \beta_1, \beta_2$ and $\beta_3 \le 1$.

In Figure 2, we plot the phase curves of the integer-order and fractional Rössler chaotic system (21) by means of the suggested scheme with initial conditions $x_0 = 0.25$, $y_0 = 0.2$,

Table 1: Comparison of $\mathscr{E}_M$, $\mathscr{C}_{h,M}$, and computational times (sec) of $\mathscr{J}^{\beta}_{0,t}[\pi t \sin(\pi t)]$, for the IM [45] and proposed schemes, when $\beta = \{0.4, 0.7, 0.9\}$ and step sizes $\hbar = \{0.01, 0.005, 0.002\}$ in $t \in [0, 1]$.

β	Step size	IM scheme			Proposed solver		
		$\mathscr{E}_M$	$\mathscr{C}_{h,M}$	CPU time	$\mathscr{E}_M$	$\mathscr{C}_{h,M}$	CPU time
0.4	0.01	2.49×10^{-3}	1.30	1.375	7.86×10^{-5}	2.05	0.610
	0.005	9.50×10^{-4}	1.31	4.843	2.00×10^{-5}	2.04	1.906
	0.002	3.62×10^{-4}	1.32	19.468	5.18×10^{-6}	2.03	7.203
0.7	0.01	2.57×10^{-4}	1.79	1.297	5.16×10^{-5}	2.14	0.641
	0.005	8.17×10^{-5}	1.78	4.937	1.29×10^{-5}	2.13	1.922
	0.002	2.58×10^{-5}	1.76	19.109	3.32×10^{-6}	2.11	7.359
0.9	0.01	3.17×10^{-5}	2.25	1.344	3.67×10^{-5}	2.22	0.609
	0.005	9.09×10^{-6}	2.19	4.703	9.10×10^{-6}	2.19	1.859
	0.002	2.59×10^{-6}	2.14	19.641	2.27×10^{-6}	2.17	7.234

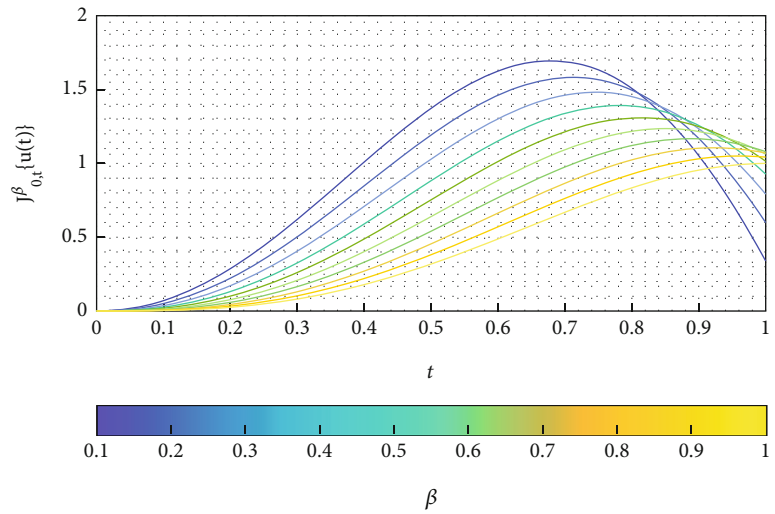

Figure 1: Comparison of the numerical results for Equation (19) applying the proposed scheme for $\beta = \{0.1, 0.2, \cdots, 1\}$ with step size $\hbar = 0.01$.

and $z_0 = 0.2$ for $\beta_3 = 0.8$ and $\beta_1 = 0.96$, $\beta_2 = 0.9$, and $\theta = 8$ with step size $\hbar = 0.002$ and $T = 100$.

We can rewrite system (21) into the following system:

$$\begin{aligned} {}^{C}\mathscr{D}^{\beta}_{0,t}u(t) &= Au(t) + \Psi(t), \\ u(0) &= u_0, \end{aligned} \tag{22}$$

where $\beta = (\beta_1, \beta_2, \beta_3)$, $u(t) = [x(t), y(t), z(t)]^T$,

$$A = \begin{bmatrix} 0 & -1 & -1 \\ 1 & \alpha & 0 \\ 0 & 0 & \theta \end{bmatrix}, \tag{23}$$

and $\Psi(t) = [0, 0, -x(t)z(t) + \chi]^T$.

Hence, the fractional impulsive control of chaotic system (22) is defined as

$$\begin{aligned} &{}^{C}\mathscr{D}^{\beta}_{0,t}u(t) = Au(t) + \Psi(t), \quad t \in \Upsilon' := \Upsilon \setminus \{t_1, t_2, \cdots, t_i\}, \quad \Upsilon := [0, T], \\ &\Delta u(t) = u(t_n^+) - u(t_n) = B(u(t_n)), \quad n = 1, 2, \cdots, i, \\ &u(0^+) = u_0, \end{aligned} \tag{24}$$

where $B = \text{diag}(-0.58, -0.68, -0.78)$ with initial conditions

$$x(0^+) = 0.25, \quad y(0^+) = 0.2, \quad z(0^+) = 0.2. \tag{25}$$

System (24) with the nonfractional term, i.e., for $\beta = (1, 1, 1)$, and fractional term was studied in [47–49].

In Figure 3, we depict the numerical approximations of system (24) by using the suggested method with the

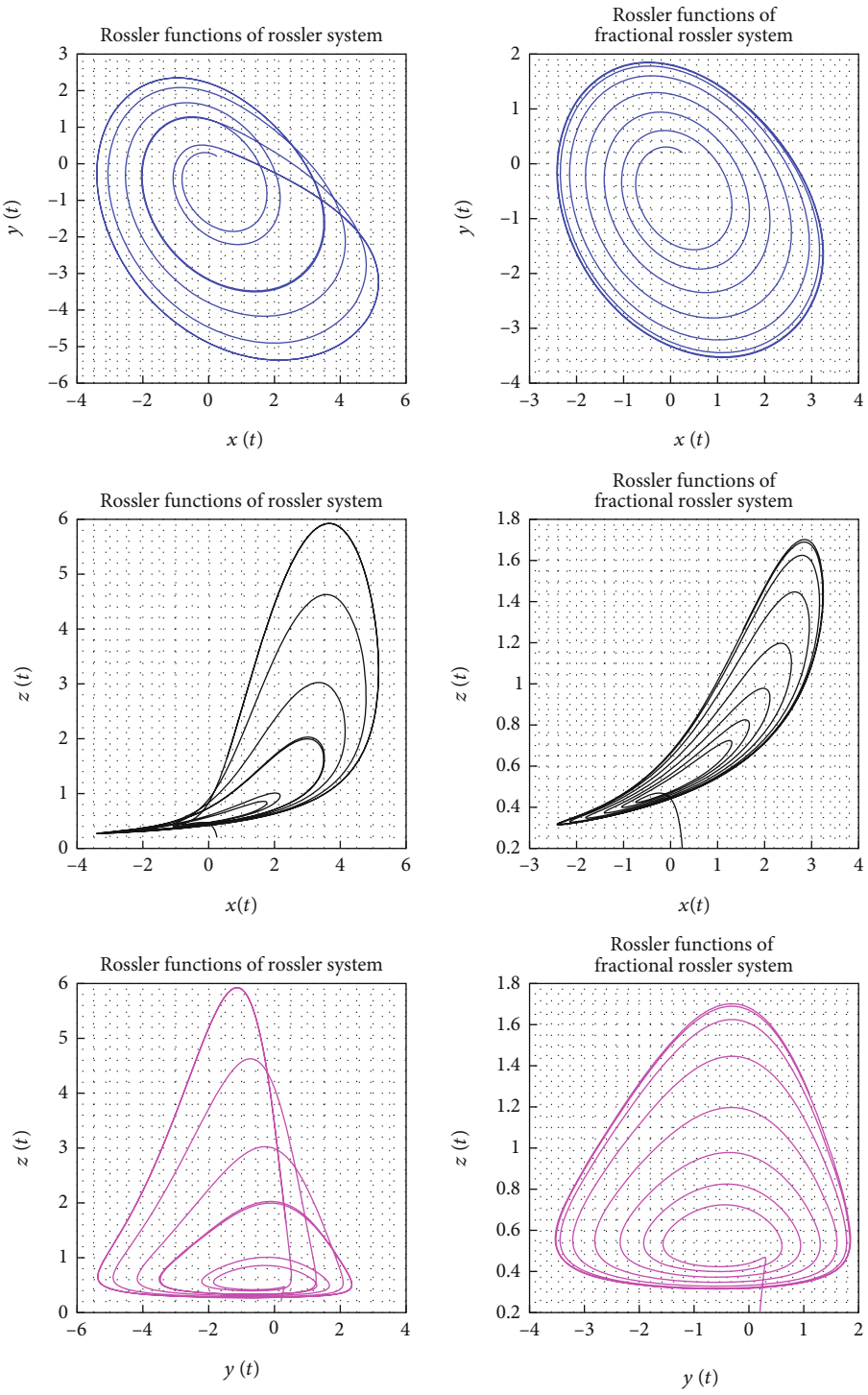

FIGURE 2: Phase curves of the integer-order ($\mathbf{L}: \beta_1 = \beta_2 = \beta_3 = 1$) and fractional ($\mathbf{R}: \beta_1 = 0.96, \beta_2 = 0.9, \beta_3 = 0.8$) Rössler chaotic systems for $\alpha = 0.4$, $\chi = 2$, and $\theta = 8$ with step size $\hbar = 0.02$ and $T = 100$.

impulsive intervals $\tau = 0.01$, in the interval $t \in [0, 10]$ and step size $\hbar = 0.002$ for $\beta_1 = 0.96$, $\beta_2 = 0.9$, and $\beta_3 = 0.8$. We can view the effects of the impulsive behaviors on this system for $\theta = 4$ in these figures.

Application 4. Assume that the functions $S(t)$, $E(t)$, and $I(t)$ denote susceptible, exposed, and infectious pests densities at time t, respectively. Furthermore, the η defines the death rate of exposed and infectious pests. The fractional susceptible-exposed-infectious (SEI) chaotic system is stated as

$$ {}^{C}\mathscr{D}_{0,t}^{\beta_1} S(t) = cS(t)\left(1 - \frac{S(t)}{K}\right) - \frac{lS(t)I(t)}{1 + nS(t)}, $$

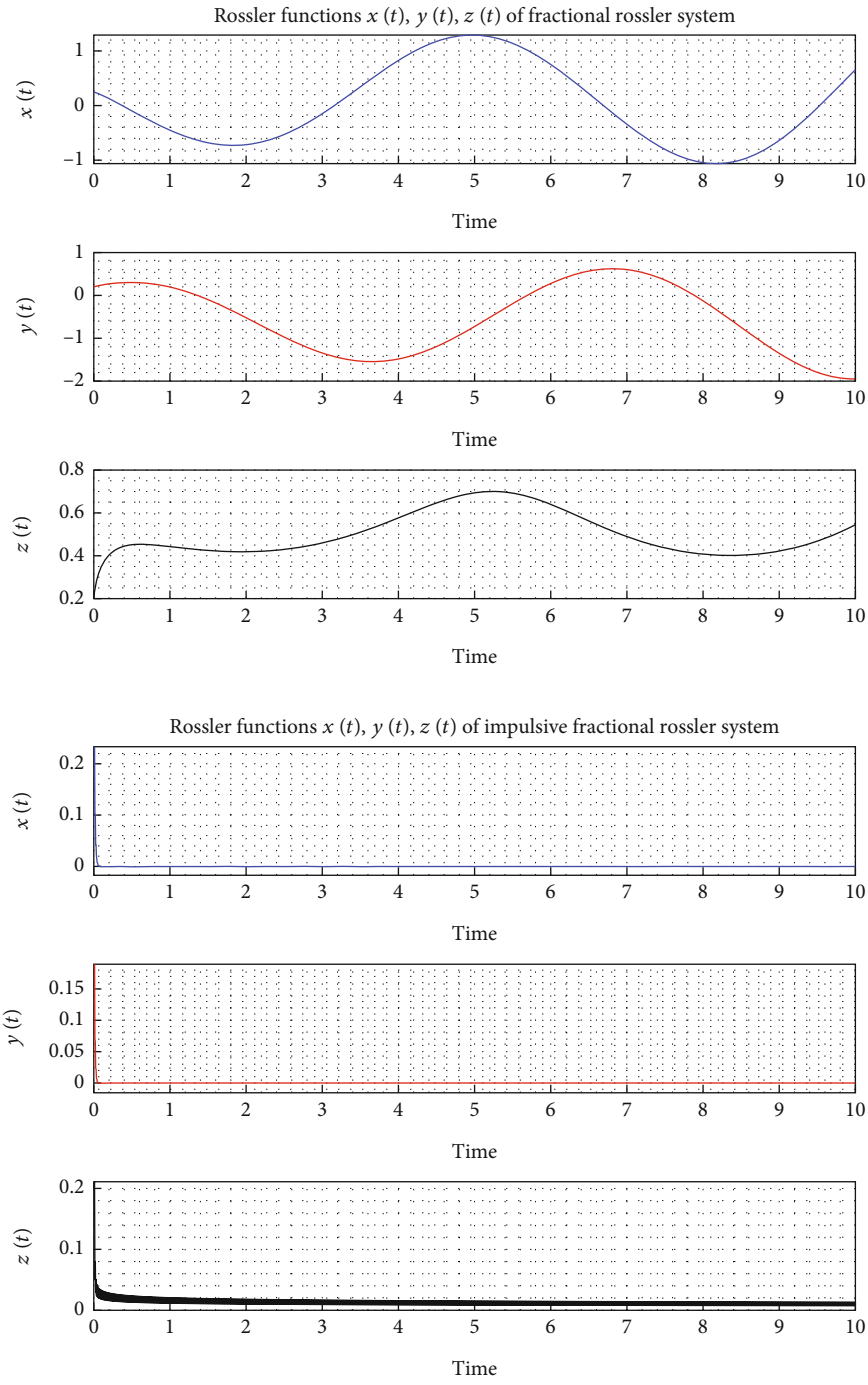

FIGURE 3: Numerical results of fractional Rössler system without and with, $\tau = 0.01$, impulsive effects for $\alpha = 0.4$, $\chi = 2$, and $\theta = 4$, based on the presented scheme for $\beta_1 = 0.96$, $\beta_2 = 0.92$, and $\beta_3 = 0.80$ with step size $\hbar = 0.005$ and $T = 10$.

$$
\begin{aligned}
{}^{C}\mathscr{D}_{0,t}^{\beta_2} E(t) &= \frac{lS(t)I(t)}{1 + nS(t)} - (\phi + \eta)E(t), \\
{}^{C}\mathscr{D}_{0,t}^{\beta_3} I(t) &= \phi E(t) - \eta I(t), \\
S(0) = S_0, E(0) &= E_0, I(0) = I_0,
\end{aligned} \tag{26}
$$

where $0 < \beta_1, \beta_2$ and $\beta_3 \leq 1$. Moreover, $S(t)$ grows logistically with a carrying capacity K in the absence of $I(t)$ and with an intrinsic birth rate constant rc.

In Figure 4, we plot the phase curves of the integer-order and fractional SEI system (26) by means of the suggested scheme with initial conditions $x_0 = 0.1$, $y_0 = 0.2$, and $z_0 = 0.3$, plus $c = 1, K = 4, d = 1.2, \phi = 0.8, n = 0.2$, and $\eta = 0.2$ for $\beta_1 = 1$, $\beta_2 = 0.9$, and $\beta_3 = 0.9$ with step size $\hbar = 0.005$ and $T = 100$.

We can rewrite system (26) into the following system:

$$
\begin{aligned}
{}^{C}\mathscr{D}_{0,t}^{\beta} u(t) &= Au(t) + \Psi(t), \\
u(0) &= u_0,
\end{aligned} \tag{27}
$$

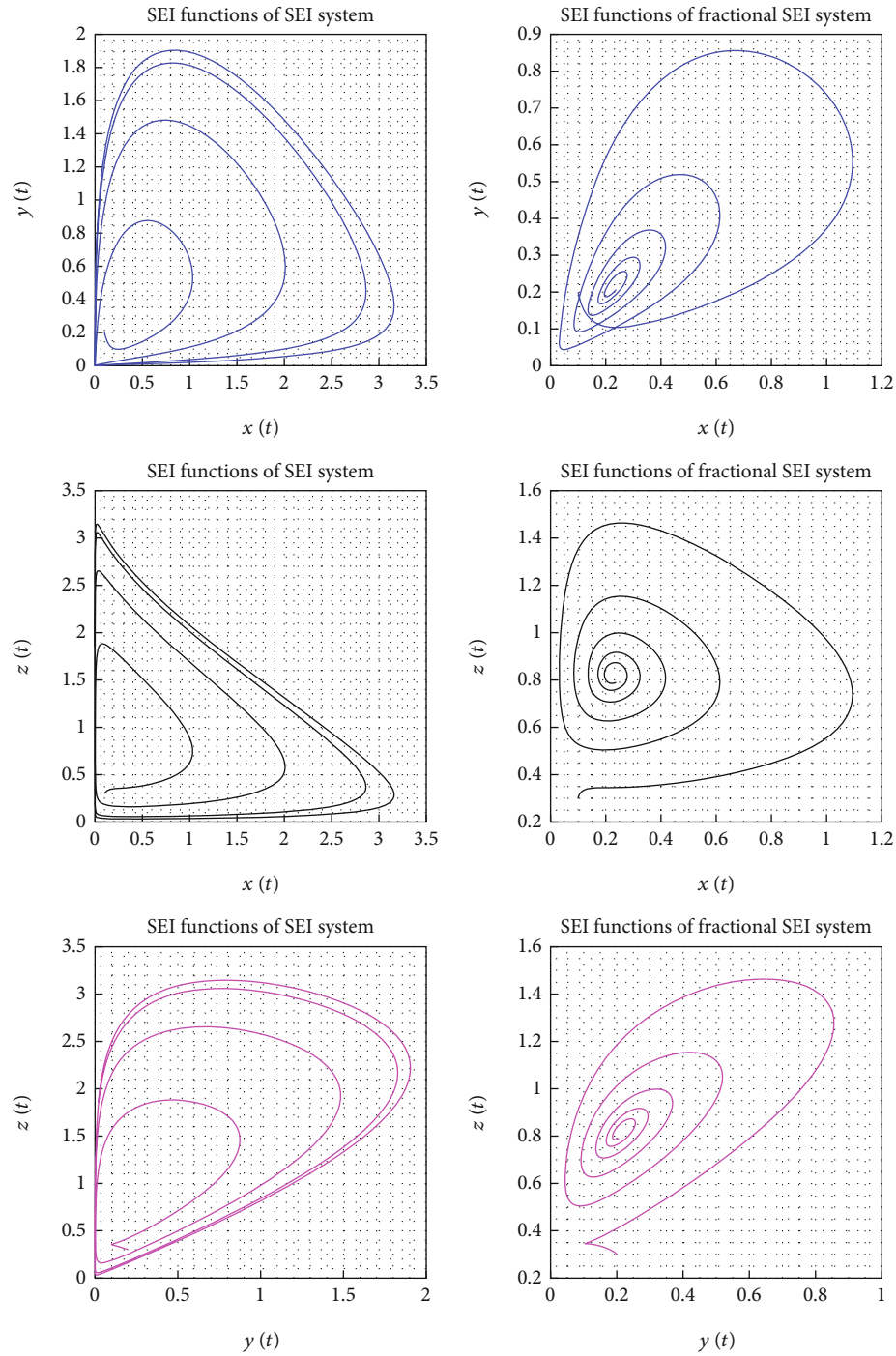

FIGURE 4: Phase curves of the integer-order ($\boldsymbol{L}$: $\beta_1 = \beta_2 = \beta_3 = 1$) and fractional ($\boldsymbol{R}$: $\beta_1 = 0.99, \beta_2 = 0.90, \beta_3 = 0.70$) SEI chaotic systems with step size $\hbar = 0.005$ and $T = 100$.

where $\beta = (\beta_1, \beta_2, \beta_3)$, $u(t) = [x(t), y(t), z(t)]^T$,

$$A = \begin{bmatrix} c & 0 & 0 \\ 0 & -(\alpha + \eta) & 0 \\ 0 & \alpha & -\eta \end{bmatrix},$$

$$\Psi(t) = \begin{bmatrix} -\left(\frac{c}{K}S(t) - \frac{l}{1 + nS(t)}I(t)\right)S(t) \\ \left(\frac{l}{1 + nS(t)}I(t)\right)S(t) \\ 0 \end{bmatrix}. \quad (28)$$

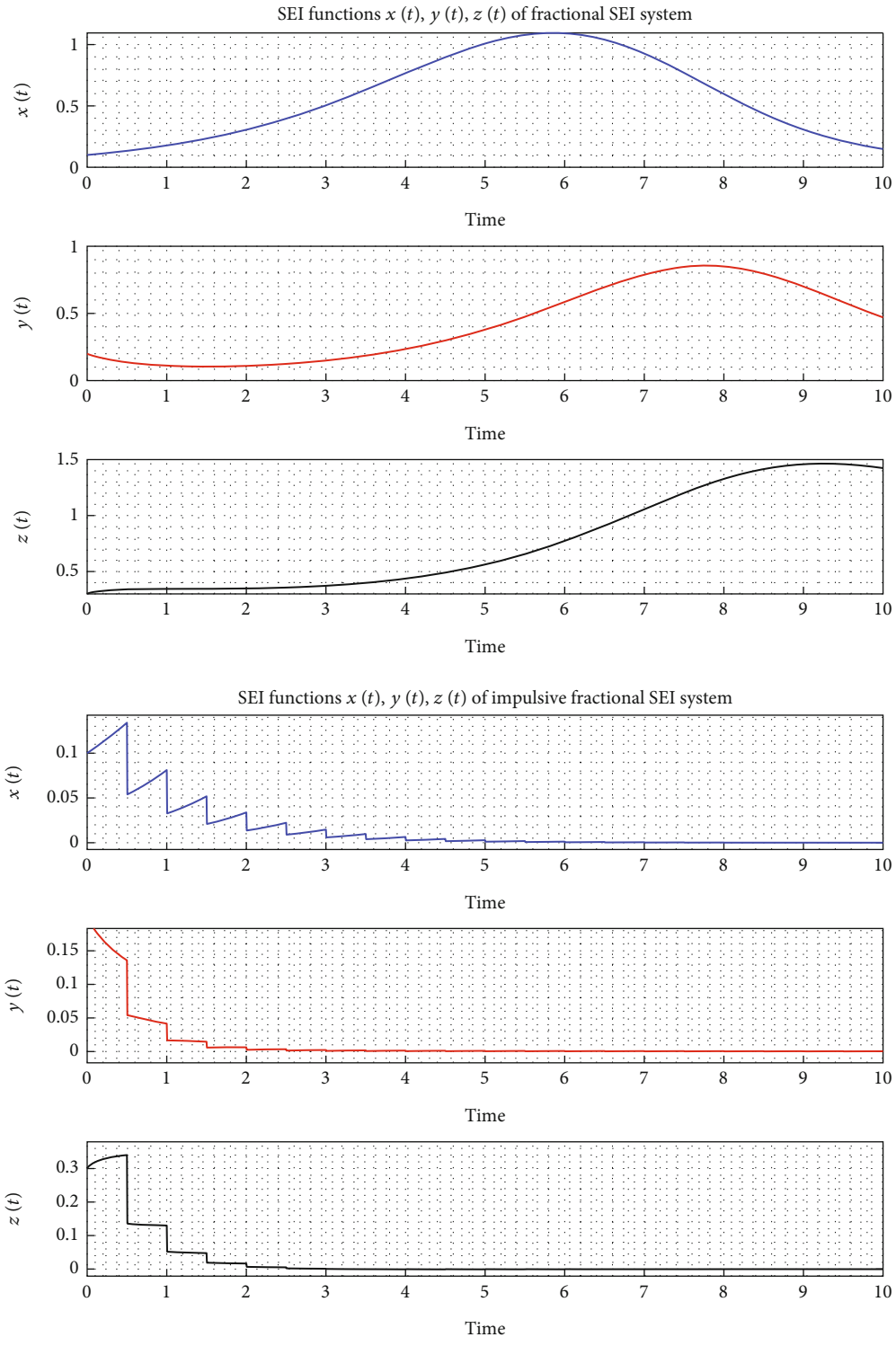

FIGURE 5: Numerical results of the fractional SEI system without and with, $\tau = 0.5$, impulsive effects based on the presented scheme for $\beta_1 = 0.99$, $\beta_2 = 0.90$, and $\beta_3 = 0.70$, with step size $\hbar = 0.005$ and $T = 10$.

Hence, the fractional impulsive control of chaotic system (27) is defined as

$$\begin{aligned} {}^{C}\mathscr{D}^{\beta}_{0,t} u(t) &= Au(t) + \Psi(t), \quad t \in \Upsilon' := \Upsilon \setminus \{t_1, t_2, \cdots, t_i\}, \\ \Delta u(t) &= u(t_n^+) - u(t_n) = B(u(t_n)), \quad n = 1, 2, \cdots, i, \\ u(0^+) &= u_0, \end{aligned} \tag{29}$$

where $Y := [0, T]$, $B = \text{diag}\,(-0.6, -0.6, -0.6)$ with initial conditions

$$\begin{aligned} x(0^+) &= 0.25, \\ y(0^+) &= 0.2, \\ z(0^+) &= 0.2. \end{aligned} \tag{30}$$

System 24 with the nonfractional term, i.e., for $\beta = (1, 1, 1)$, was studied in [50].

In Figure 5, we depict the numerical approximations of systems (26) and (29) by using the suggested method with the impulsive intervals $\tau = 0.5$, in the interval $t \in [0,100]$ and step size $\hbar = 0.005$ for $\beta_1 = 0.99$, $\beta_2 = 0.90$, and $\beta_3 = 0.70$. We can view the effects of the impulsive behaviors on this system in these figures.

4. Conclusion

In the framework of this study, an implicit numerical algorithm for computing the approximate solutions of fractional impulsive differential equations was presented. This numerical solver relies on the B-spline interpolation to reasonably approximate the nonlocal integral operators. An illustrative example showed the accuracy of the comparison of the results obtained by the IM scheme and proposed numerical technique. The results confirmed the superiority of the presented scheme. Then, the proposed algorithm for solving the fractional chaotic dynamic Rössler and SEI systems was applied, and the results were studied using phase figures. To top it all off, the fractional impulsive systems were approximated by the presented method, and the achievement results of the impulsive behavior were analyzed.

Data Availability

There is no underlying data supporting the results in this study.

Conflicts of Interest

The authors declare that they have no known competing financial interests or personal relationships that could have appeared to influence the work reported in this paper.

References

[1] V. Lakshmikantham and P. S. Simeonov, "Theory of impulsive differential equations," vol. 6, World Scientific, 1989.

[2] M. Benchohra, J. Henderson, and S. Ntouyas, *Impulsive Differential Equations and Inclusions*, vol. 2, Hindawi Publishing Corporation New York, 2006.

[3] G. T. Stamov, *Almost Periodic Solutions of Impulsive Differential Equations*, vol. 2047, Springer Science & Business Media, 2012.

[4] I. Stamova and G. Stamov, "Stability analysis of impulsive functional systems of fractional order," *Communications in Nonlinear Science and Numerical Simulation*, vol. 19, no. 3, pp. 702–709, 2014.

[5] I. Stamova and G. Stamov, *Applied Impulsive Mathematical Models*, Springer International Publishing, 2016.

[6] S. Sun and L. Chen, "Dynamic behaviors of Monod type chemostat model with impulsive perturbation on the nutrient concentration," *Journal of Mathematical Chemistry*, vol. 42, no. 4, pp. 837–847, 2007.

[7] S. Ahmad and G. T. Stamov, "On almost periodic processes in impulsive competitive systems with delay and impulsive perturbations," *Nonlinear Analysis: Real World Applications*, vol. 10, no. 5, pp. 2857–2863, 2009.

[8] J. Yang and Z. Yang, "Stability and permanence of a pest management model with impulsive releasing and harvesting," *Abstract and Applied Analysis*, vol. 2013, Article ID 832701, 18 pages, 2013.

[9] E. Joelianto and H. Y. Sutarto, "Controlled switching dynamical systems using linear impulsive differential equations," in *Intelligent Unmanned Systems: Theory and Applications*, pp. 227–244, Springer, Berlin Heidelberg, 2009.

[10] Y. Zhao, Y. Xia, and W. Ding, "Periodic oscillation for BAM neural networks with impulses," *Journal of Applied Mathematics and Computing*, vol. 28, no. 1-2, pp. 405–423, 2008.

[11] C. Wang, "Piecewise pseudo-almost periodic solution for impulsive non-autonomous high- order Hopfield neural networks with variable delays," *Neurocomputing*, vol. 171, pp. 1291–1301, 2016.

[12] T. Jankowski, "Positive solutions to second order four-point boundary value problems for impulsive differential equations," *Applied Mathematics and Computation*, vol. 202, no. 2, pp. 550–561, 2008.

[13] W. Wang and X. Yang, "Positive periodic solutions for second order differential equations with impulsive effects," *Boundary Value Problems*, vol. 2015, no. 1, 2015.

[14] Q. Wang and M. Wang, "Existence of solution for impulsive differential equations with indefinite linear part," *Applied Mathematics Letters*, vol. 51, pp. 41–47, 2016.

[15] X. Yang, "Existence and multiplicity of weak solutions for a nonlinear impulsive (q,p)-Laplacian dynamical system," *Advances in Difference Equations*, vol. 2017, no. 1, 2017.

[16] H. Chen and J. Sun, "An application of variational method to second-order impulsive differential equation on the half-line," *Applied Mathematics and Computation*, vol. 217, no. 5, pp. 1863–1869, 2010.

[17] H. Hossainzadeh, G. A. Afrouzi, and A. Yazdani, "Application of Adomian decomposition method for solving impulsive differential equations," *Journal of Mathematics and Computer Science*, vol. 2, no. 4, pp. 672–681, 2011.

[18] Z. Yang, "The asymptotic behavior for a class of impulsive delay differential equations," *Abstract and Applied Analysis*, vol. 2013, Article ID 494067, 7 pages, 2013.

[19] Z. Zhang and H. Liang, "Collocation methods for impulsive differential equations," *Applied Mathematics and Computation*, vol. 228, pp. 336–348, 2014.

[20] M. Berenguer, H. Kunze, D. L. Torre, and M. R. Gal'an, "Galerkin method for constrained variational equations and a collage-based approach to related inverse problems," *Journal of Computational and Applied Mathematics*, vol. 292, pp. 67–75, 2016.

[21] L. Mei, H. Sun, and Y. Lin, "Numerical method and convergence order for second-order impulsive differential equations," *Advances in Difference Equations*, vol. 2019, no. 1, 2019.

[22] Y. Zhou, J. Wang, and L. Zhang, *Basic Theory of Fractional Differential Equations*, World Scientific, 2016.

[23] R. Karimi, A. Dabiri, J. Cheng, and E. A. Butcher, "Probabilistic-robust optimal control for uncertain linear time-delay systems by state feedback controllers with memory," in *2018 Annual American Control Conference (ACC)*, pp. 4183–4188, Milwaukee, WI, USA, 2018.

[24] B. P. Moghaddam, A. Dabiri, and J. A. T. Machado, "Application of variableorder fractional calculus in solid mechanics," in

Applications in Engineering, Life and Social Sciences, D. Băleanu and A. M. Lopes, Eds., pp. 207–224, Part A, De Gruyter, 2019.

[25] V. Erturk, E. Godwe, D. Baleanu, P. Kumar, J. Asad, and A. Jajarmi, "Novel fractional-order Lagrangian to describe motion of beam on nanowire," *Acta Physica Polonica A*, vol. 140, no. 3, pp. 265–272, 2021.

[26] A. Jajarmi, D. Baleanu, K. Z. Vahid, H. M. Pirouz, and J. Asad, "A new and general fractional Lagrangian approach: a capacitor microphone case study," *Results in Physics*, vol. 31, article 104950, 2021.

[27] B. P. Moghaddam, M. Pishbin, Z. S. Mostaghim, O. S. Iyiola, A. Galhano, and A. M. Lopes, "A numerical algorithm for solving nonlocal nonlinear stochastic delayed systems with variable-order fractional Brownian noise," *Fractal and Fractional*, vol. 7, no. 4, p. 293, 2023.

[28] Z. S. Mostaghim, B. P. Moghaddam, and H. S. Haghgozar, "Computational technique for simulating variable-order fractional Heston model with application in US stock market," *Mathematical Sciences*, vol. 12, no. 4, pp. 277–283, 2018.

[29] Z. S. Mostaghim, B. P. Moghaddam, and H. S. Haghgozar, "Numerical simulation of fractional-order dynamical systems in noisy environments," *Computational and Applied Mathematics*, vol. 37, no. 5, pp. 6433–6447, 2018.

[30] C. Ionescu, A. Lopes, D. Copot, J. A. T. Machado, and J. H. T. Bates, "The role of fractional calculus in modeling biological phenomena: a review," *Communications in Nonlinear Science and Numerical Simulation*, vol. 51, pp. 141–159, 2017.

[31] D. Baleanu, F. A. Ghassabzade, J. J. Nieto, and A. Jajarmi, "On a new and generalized fractional model for a real cholera outbreak," *Alexandria Engineering Journal*, vol. 61, no. 11, pp. 9175–9186, 2022.

[32] D. Baleanu, M. H. Abadi, A. Jajarmi, K. Z. Vahid, and J. Nieto, "A new comparative study on the general fractional model of COVID-19 with isolation and quarantine effects," *Alexandria Engineering Journal*, vol. 61, no. 6, pp. 4779–4791, 2022.

[33] H. Xi, S. Yu, R. Zhang, and L. Xu, "Adaptive impulsive synchronization for a class of fractional-order chaotic and hyperchaotic systems," *Optik*, vol. 125, no. 9, pp. 2036–2040, 2014.

[34] D. Li, X. P. Zhang, Y. T. Hu, and Y. Y. Yang, "Adaptive impulsive synchronization of fractional order chaotic system with uncertain and unknown parameters," *Neurocomputing*, vol. 167, pp. 165–171, 2015.

[35] X. Zhang, D. Li, and X. Zhang, "Adaptive impulsive synchronization for a class of fractional order complex chaotic systems," *Journal of Vibration and Control*, vol. 25, no. 10, pp. 1614–1628, 2019.

[36] J. Fu, M. Yu, and T.-D. Ma, "Modified impulsive synchronization of fractional order hyperchaotic systems," *Chinese Physics B*, vol. 20, no. 12, article 120508, 2011.

[37] M. S. Ali, G. Narayanan, V. Shekher, A. Alsaedi, and B. Ahmad, "Global Mittag-Leffler stability analysis of impulsive fractional-order complex-valued BAM neural networks with time varying delays," *Communications in Nonlinear Science and Numerical Simulation*, vol. 83, article 105088, 2020.

[38] M. Feckan, Y. Zhou, and J. Wang, "On the concept and existence of solution for impulsive fractional differential equations," *Communications in Nonlinear Science and Numerical Simulation*, vol. 17, no. 7, pp. 3050–3060, 2012.

[39] Y. Qiao and Z. Zhou, "Existence of solutions for a class of fractional differential equations with integral and anti-periodic boundary conditions," *Boundary Value Problems*, vol. 2017, no. 1, 2017.

[40] Y. Guan, Z. Zhao, and X. Lin, "On the existence of solutions for impulsive fractional differential equations," *Advances in Mathematical Physics*, vol. 2017, Article ID 1207456, 12 pages, 2017.

[41] Q. Chen, A. Debbouche, Z. Luo, and J. Wang, "Impulsive fractional differential equations with Riemann-Liouville derivative and iterative learning control," *Chaos, Solitons & Fractals*, vol. 102, pp. 111–118, 2017.

[42] S. G. Samko, A. A. Kilbas, and O. I. Marichev, *Fractional Integrals and Derivatives: Theory and Applications*, Gordon & Breach Science Publishers, 1993.

[43] M. Caputo, "Linear models of dissipation whose Q is almost frequency independent-II," *Geophysical Journal International*, vol. 13, no. 5, pp. 529–539, 1967.

[44] M. Caputo, *Elasticit'a e dissipazione*, Zanichelli, Bologna, Italy, 1969.

[45] F. K. Keshi, B. P. Moghaddam, and A. Aghili, "A numerical approach for solving a class of variable-order fractional functional integral equations," *Computational and Applied Mathematics*, vol. 37, no. 4, pp. 4821–4834, 2018.

[46] B. P. Moghaddam, A. Dabiri, Z. S. Mostaghim, and Z. Moniri, "Numerical solution of fractional dynamical systems with impulsive effects," *International Journal of Modern Physics C*, vol. 34, no. 1, 2023.

[47] J. Sun and Y. Zhang, "Impulsive control of Rossler systems," *Physics Letters A*, vol. 306, no. 5-6, pp. 306–312, 2003.

[48] L. Yang, L. Xiao-Feng, L. Chuan-Dong, and C. Guo, "Impulsive control for synchronization of nonlinear Rössler chaotic systems," *Chinese Physics*, vol. 15, no. 12, pp. 2890–2893, 2006.

[49] A. Razminia, V. J. Majd, and D. Baleanu, "Chaotic incommensurate fractional order Rössler system: active control and synchronization," *Advances in Difference Equations*, vol. 2011, no. 1, 2011.

[50] Z. Xiang, Y. Li, and X. Song, "Dynamic analysis of a pest management SEI model with saturation incidence concerning impulsive control strategy," *Nonlinear Analysis: Real World Applications*, vol. 10, no. 4, pp. 2335–2345, 2009.